



Design of Composite Disc Spring for Automotive Suspension with using Numerical Simulation

Martin Mrazek, Michal Skovajsa, Frantisek Sedlacek (0000-0003-1678-149X)

Faculty of Mechanical Engineering, University of West Bohemia in Pilsen. Univerzitni 8, 300 01 Plzen. Czech Republic. E-mail: mrma@kks.zcu.cz, skovi@kks.zcu.cz, fsedlace@kks.zcu.cz

Article abstract

This paper investigates the replacement of a conventional steel coil spring with a composite disc spring with the aim of minimizing its weight. Simulation in the CAD system Siemens NX 12 was used to determine the composite disc spring's behavior. The regression functions were stated based on the numerical simulation. Based on the regression functions the solution with the minimum weight was found using software programmed in Matlab. The prototype discs were manufactured from carbon fibre prepreg. Their load-deflection characteristics were tested and compared with the designed values. The experimental results show that using this solution reduces the weight by about 30% in this case.

Keywords

carbon fibre
composite material
disc spring
optimization

DOI

10.21062/mft.2021.100

Available online

December 17, 2021

1 Introduction

There is a Europe-wide trend to reduce CO₂ emissions in road vehicles. One of the ways to reduce CO₂ emissions is to make a vehicle lighter. Coil springs are used in many automotive applications. They are made of steel and have a high total weight. Coil springs are often dynamically loaded and if they are made from steel there is no way to reduce the weight much.

Many authors [7][8][9] investigate mathematical modelling of composites disc springs and the theoretical application. There is no study of replacing conventional steel coil springs with composites disc springs focused to weight in the real situation. The manufacture process of disc spring is relatively simple it could be manufactured in prototype production with acceptable cost. Additionally, disc springs allow a large range of non-linear load-deflection curves and spring rates to be achieved. This is done by stacking of disc springs in series and parallel, offering further means to obtain desired stiffness variation [7].

This paper investigates the possibility of replacing the steel coil spring with carbon fibre composite disc springs to minimize weight. The damper with steel coil spring (ZF Formula Student) was chosen for this case study.

2 Case study

The coil spring of the damper is made from EN 10270-1 steel with linear load-deflection curve. The damper with the spring is shown in Fig. 1. The weight of one spring is 0.372 kg. The spring must provide a minimum compression of 35 mm. It is depended on suspension kinematic and the rules where the minimum wheel travel is defined [1]. The limitation factor for the design of the new damper is the space where the spring can be placed. The maximum outer diameter is 70 mm, the minimum inner diameter is 42 mm and the maximum height is 147 mm.

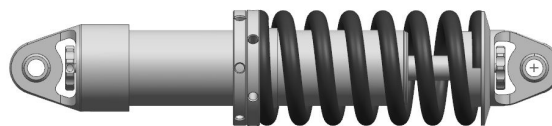


Fig. 1 Damper with the coil spring

A typical disc spring geometric parameters is shown in Fig.2. The Load-deflection curve is typically non-linear dependent to b_0/t ratio. For b_0/t ratio 0.4, 0.8 and 1.2 the load-deflection is approximately linear, medium regression, and high regression [11].

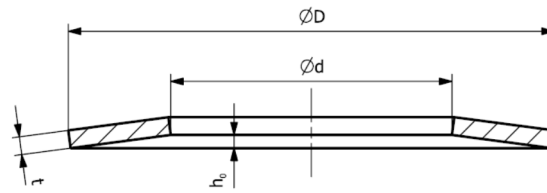


Fig. 2 Geometrical parameters of typical disc spring

3 Design of composite disk spring

Because a plate spring has low maximum compression, several disks in series are needed. Standard disc springs in a serial arrangement need a tube or a shaft to hold all the discs centred. We designed a flange on each disc to eliminate the need for this (Fig. 3).

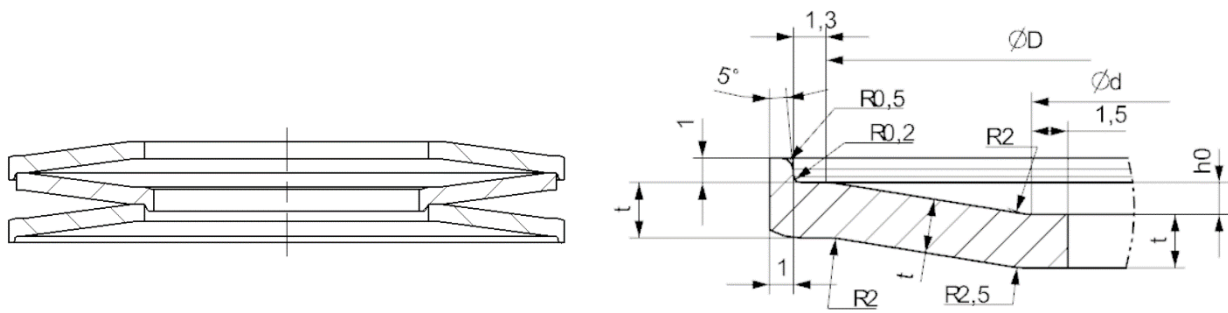


Fig. 3 The serial arrangement of discs (left); Disc with outer flange – basic dimensions (right)

If we want to make a spring from steel or other isotropic materials, we use basic relations to calculate them. Because composite materials do not exhibit isotropic behaviour, these basic relations cannot be used. Numerical simulation based on FEM and software developed in Matlab were used for finding the basic dimensions of the springs and number of the discs. The spring behavior was described by regression functions. FEM analysis was used to determine the regression coefficients and Matlab software to search for a low-weight solution which corresponds to the defined conditions [13].

FEM analysis was performed on a disc which has a flange on the outer diameter side. On the model surface was applied mesh with a second order quadratic elements (type CQUAD8) [3]. The centre point of the disc and the inner edge was connected by a 1D connection (RBE3 elements). Fig. 4 shows the boundary conditions which were applied on the outer edge and the centre point. The load was applied to the centre point as a z-direction displacement.

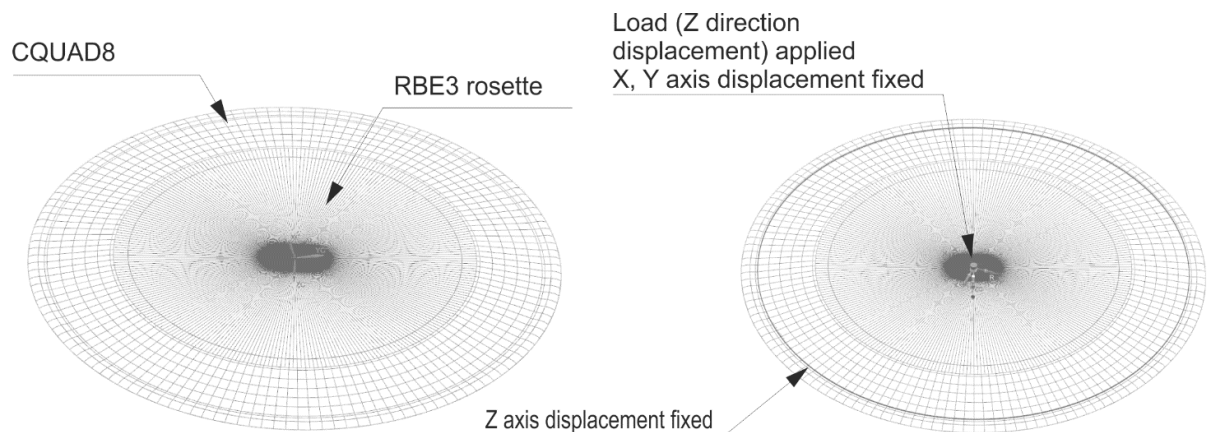


Fig. 4 Specimen of mesh (left); Boundary conditions (right)

The carbon fibre prepreg GG200t – twill 2x2 with epoxy matrix was used [12]. The mechanical properties used material for numeric simulation are given in Tab. 1.

Tab. 1 Carbon fibre prepreg GG200t mechanical properties

t (mm)	0.203	Thickness of the ply	
ρ (kg/m ³)	1570	Density	
E_1 (GPa)	55.8	Young's Modulus 0°	acc. to ASTM D 3039
E_2 (GPa)	53.7	Young's Modulus 90°	acc. to ASTM D 3039
E_3 (GPa)	6.4	Young's Modulus N90°	acc. to ASTM D 3039
G_{12} (GPa)	5.29	In-plane Shear Modulus	acc. to ASTM D 3518
ν_{12} (-)	0.27	Major Poisson's Ratio	acc. to ASTM D 3039

The maximum stress failure criterion was used to evaluate the strength of the spring. According to this theory, failure occurs when any stress component reaches the ultimate strength of the material [2]. The maximum stress criterion and maximum strength values are shown in Tab. 2.

Tab. 2 Maximum stress criterion (left); Maximum strength value for carbon fibre GG200t

Failure indexes	Maximum stress criterion			
F_{11}	σ_1/X^T if $\sigma_1 > 0$; σ_1/X^C if $\sigma_1 < 0$	X^T (MPa)	693	Tensile strength (0°)
F_{22}	σ_2/Y^T if $\sigma_2 > 0$; σ_2/Y^C if $\sigma_2 < 0$	Y^T (MPa)	610	Tensile strength (90°)
F_{33}	σ_3/Z^T if $\sigma_3 > 0$; σ_3/Z^C if $\sigma_3 < 0$	Z^T (MPa)	67	Tensile strength (N90°)
F_{12}	$ \tau_{12}/S_{12} $	X^C (MPa)	552	Compression strength (0°)
F_{23}	$ \tau_{23}/S_{23} $	Y^C (MPa)	558	Compression strength (90°)
F_{13}	$ \tau_{13}/S_{13} $	Z^C (MPa)	268	Compression strength (N90°)
F_{IL}	$\sqrt{\left(\frac{\tau_{13}}{S_{13}}\right)^2 + \left(\frac{\tau_{23}}{S_{23}}\right)^2}$	S_{12} (MPa)	109.1	In-Plane Shear Strength
		S_{ILSS} (MPa)	67.7	In-Lam. Shear Strength

Tab. 3 shows the dimensions of the discs and calculated values that were necessary for the regression function. The inner diameter d was constant 48 mm, the outer diameter D was expected in the range 60 – 70 mm, the height-thickness ratio h_0/t was expected in the range 0.5 – 0.8, the thickness was expected from 1,5 mm to 3 mm, the maximum deflection was expected from 60 % to 95 %.

Tab. 3 Dimensions of the disc and calculated values

d	D	h_0/t	t	S_p	F_z	F_I
[mm]	[mm]	[-]	[mm]	[%]	[N]	[-]
48	70	0.5	1.5	60	201	0.155
48	70	0.5	1.5	95	318	0.247
48	70	0.5	3	60	2990	0.592
48	70	0.5	3	95	4736	0.937
48	70	0.8	1.5	60	435	0.298
48	70	0.8	1.5	95	689	0.47
48	70	0.8	3	60	6311	1.129
48	70	0.8	3	95	9993	1.787
48	60	0.5	1.5	60	460	0.268
48	60	0.5	1.5	95	729	0.425
48	60	0.5	3	60	6332	0.98
48	60	0.5	3	95	10026	1.558
48	60	0.8	1.5	60	1027	0.516
48	60	0.8	1.5	95	1626	0.817
48	60	0.8	3	60	8281	1.235
48	60	0.8	3	95	13112	1.955

The general form of the regression function for reaction force is

$$F_z = b_0 \cdot \left(\frac{h_0}{t} \right)^{b_1} \cdot t^{b_2} \cdot s_p^{b_3} \cdot D^{b_4}, \quad (1)$$

and the general form of the regression function for failure index calculation is

$$F_I = c_0 \cdot \left(\frac{h_0}{t} \right)^{c_1} \cdot t^{c_2} \cdot s_p^{c_3} \cdot D^{c_4}, \quad (2)$$

and the regression constants were calculated based on Tab. 3. The final formulas are

$$F_z = 240507 \cdot \left(\frac{h_0}{t} \right)^{0.868037} \cdot t^{3.39526} \cdot s_p^{1.00014} \cdot D^{-2.67542}, \quad (3)$$

$$F_I = 3.17252 \cdot \left(\frac{h_0}{t} \right)^{0.861713} \cdot t^{1.61125} \cdot s_p^{1.00126} \cdot D^{-1.59992}. \quad (4)$$

The regression constants show that the reaction force and failure index have almost linear dependence on the disc compression. The reaction force is mostly dependent on the disc thickness. The failure index has a negative dependency on the outer disc diameter.

Tab. 4 Matlab boundary conditions

Parameter	Condition	Description
m [kg]	min	Weight
F_I [-]	< 0.9	Failure index
k [N mm ⁻¹]	$80 - 90$	Stiffness
d [mm]	48	Inner diameter
s [mm]	$s < b_0$	Deflection
n [-]	$6 - 40$	Number of disc for one damper
t [mm]	$1 - 3.0$	Disc thickness
s_t [mm]	35	Damper compression

When the mathematical equation and the boundary conditions have been determined (Tab. 4) the final spring parameters can be calculated. The software in Matlab is used. The software calculates the dimensions and number of discs for one damper. The values which correspond to the boundary conditions are sorted by weight (Tab. 5).

Tab. 5 Matlab calculation result

m [kg]	F_I [-]	k [N mm ⁻¹]	n [-]	D [mm]	b_0 [mm]	t [mm]
0.27 3	0.8 7	79.1	32	64	1.21	2.2
0.27 3	0.8 7	79.0	32	64	1.23	2.2
0.27 3	0.8 6	78.8	32	64	1.25	2.2
0.27 3	0.8 6	78.6	32	64	1.28	2.2
0.27 3	0.8 6	78.4	32	64	1.30	2.2
0.27 3	0.8 6	78.2	32	64	1.32	2.2

4 Experimental testing

One pair of discs was manufactured based on the calculated data. The discs were both laminated in one mould specially designed for this experiment [5][6]. The mould was built in two parts from aluminium alloy. This solution provides high surface quality on both sides of the laminated part [4]. The laminate layup was [0/45]₆. The springs were cured in an autoclave with an external pressure of 2 bars and a temperature of 110°C. The final manufactured discs are shown in Fig. 5.



Fig. 5 Samples of manufactured springs

Both discs were compression tested to check their load-deflection behaviour. Fig. 6 and Fig. 7 shows the typical set-up for testing on the electro-mechanical testing machine Zwick/Roell Z250 . A compression test speed of 1 mm/min was used with a compression limit of 1.5 mm. Each disc was tested separately.



Fig. 6 Load-deflection testing

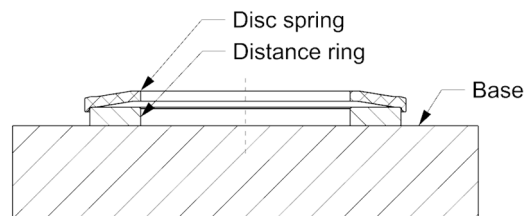


Fig. 7 Typical testing setup

The weight was measured using an analytical laboratory scale with an accuracy of 0.001 g.

The thickness was measured with a micrometre with an accuracy of 0.01 mm. Three points on each disc were measured.

Tab. 6 Discs weight

	Thick- ness [mm]	Weight [g]
Disc with outer flange	2.247	8.585
Disc with inner flange	2.257	7.947

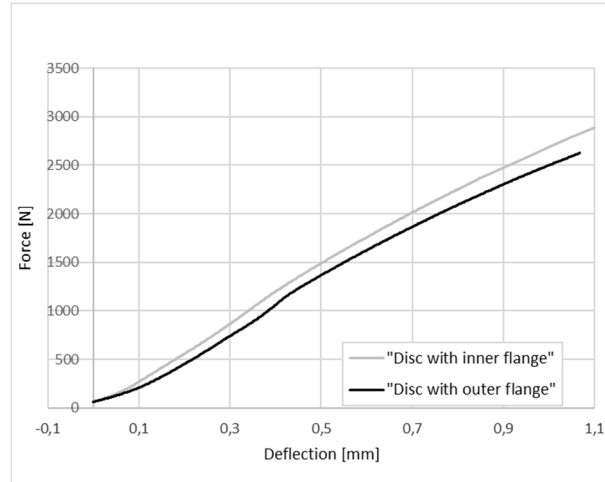


Fig. 8 Load-deflection characteristic

No.	Specimen ID	E_{mod} N/mm	F_{max} N	dL at F_{max} mm	Notes
1	01+extens.	2850	2630	1,1	E(300-2000N)
2	01+extens.	2850	2620	1,1	E(300-2000N)
3	02+extens.	2980	2890	1,1	E(300-2000N)
4	02+extens.	2980	2870	1,1	E(300-2000N)

Fig. 9 Load-deflection test results

5 Results from experimental testing and discussion

One pair of disc springs was manufactured. Tab. 6 shows the thickness of each disc. The differences between the calculated and measured thickness is about 2.5%. The weight measurement shows differences between the discs. This difference is caused by the geometrical differences between the discs. The weight of all the discs needed for the damper is 265 g. This is 107g (29 %) less than the original steel spring. If we compare this weight with the calculated value, the differences can be seen. This is due to the simplification of the calculation. In the calculation, only the spring with the outer flange was used.

Fig. 8 shows the load-deflection characteristics of the disc. The nonlinearity from the whole range was evaluated. The non-linearity of the disc with the inner flange is 2.6 %. The non-linearity of the disc with the outer flange is 8.7 %. If we calculate stiffness from maximum displacement and maximum load and divide the value by the number of discs needed for the damper, this is the same way as the calculation software did the stiffness calculation. The stiffness of the disc with the outer flange is 75 N/mm. The stiffness of the disc with the inner flange is 82N/mm. The comparison of the designed stiffness (Tab. 5) and the measured stiffness is 5.5 % for the disc with the outer flange and 3.5 % for the disc with the inner flange. The design process shows the Fig. 10.

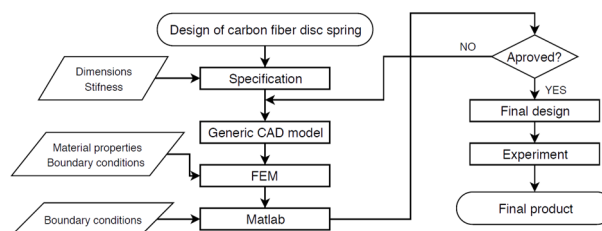


Fig. 10 Design process flowchart

6 Conclusion

This paper deals with the possibility of replacing the steel coil spring with carbon fibre composite disc springs to minimize weight. The carbon fibre disc springs were designed using FEA and Matlab software. One pair of discs was manufactured and experimentally tested. Comparison of the designed parameters and experimental testing results found a difference in stiffness of 5.5 % and 3.5 %. The designed solution is 29% lighter than the original coil spring. The designed solution shows the possibility of replacing the steel coil spring with the carbon fibre composite disc spring in this case.

Acknowledgement

The article has been prepared under project SGS-2019-030 - Research and development of Advanced Components for the Formula Student Car.

References

- [1] Formula student FSG RULES 2020. Online. 5.1.2020. www.fsg.one/rules
- [2] VASILIEV, VALERY V A MOROZOV, EVGENY V. *Advanced Mechanics of Composite Materials and Structural elements*, 3rd Edition. Oxford: Elsevier, 2013. ISBN: 978-0-08-098231-1.
- [3] O. C. ZIENKIEWICZ, R. L. TAYLOR, AND J. Z. ZHU, *The Finite Element Method: Its Basis and Fundamentals, Seventh Edition*, 7 edition. Amsterdam: Butterworth-Heinemann, 2013.
- [4] A. C. LONG, ED., *Design and Manufacture of Textile Composites*, 1 edition. Boca Raton, Fla.: Woodhead Publishing, 2005.
- [5] HYNEK, M., ŘEHOUNEK, L, VOTÁPEK, P.. Numerical analysis of production procedure of aluminium bellows by means of hydroforming. In *Metal 2013*. Ostrava: Tanger, 2013. s. 496-501. ISBN: 978-80-87294-39-0
- [6] Rusnakova S, Capka A, Fojtl L, Zaludek M, Rusnak V. Technology and Mold Design for Production of Hollow Carbon Composite Parts. *Manufacturing Technology*. 2016;16(4):799-804. doi: 10.21062/ujep/x.2016/a/1213-2489/MT/16/4/799.
- [7] Foard, J., Rollason, D., Thite, A., & Bell, C. (2019). Polymer composite Belleville springs for an automotive application. *Composite Structures*, 221, 110891. <https://doi.org/10.1016/j.compstruct.2019.04.063>
- [8] Zheng, E., Jia, F., & Zhou, X. (2014). Energy-based method for nonlinear characteristics analysis of Belleville springs. *Thin-Walled Structures*, 79, 52–61. <https://doi.org/10.1016/j.tws.2014.01.025>
- [9] Patangtalo, W., Aimmanee, S., & Chutima, S. (2016). A unified analysis of isotropic and composite Belleville springs. *Thin-Walled Structures*, 109, 285–295. <https://doi.org/10.1016/j.tws.2016.09.023>
- [10] Josh Winkler. Composite Spring Capabilities, 2018. URL: <https://www.mw-ind.com/composite-spring-capabilities/>.
- [11] Wang, W., Wang, X. Tests, model, and applications for coned-disc-spring vertical isolation bearings. *Bull Earthquake Eng* 18, 357–398 (2020). <https://doi.org/10.1007/s10518-019-00728-8>
- [12] Mañas L, Rusnáková S, Javořík J, Žaludek M, Fojtl L. Verification of Material Composition and Manufacturing Process of Carbon Fibre Wheel. *Manufacturing Technology*. 2019;19(2):280-283. doi: 10.21062/ujep/283.2019/a/1213-2489/MT/19/2/280.
- [13] Kulhavý P, Fliegel V. Experimental and Numerical Analysis of Dynamic Properties of Wound and Wrapped Carbon Composites. *Manufacturing Technology*. 2019;19(2):248-253. doi: 10.21062/ujep/278.2019/a/1213-2489/MT/19/2/248.